LncRNA Gm12664 up-regulates CAV1 expression to promote hepatocellular lipid accumulation by sponging miR-295-5p

Fei Xu[1,2], Liqiang Wang[1], Zhenfeng Song[3], Linjun Chen[1], Qingwen Zhang[1], Lixin Na[1,2,3*]

1. College of Medical Technology, Shanghai University of Medicine & Health Sciences, Shanghai 201318, China
2. Collaborative Innovation Center of Shanghai University of Medicine & Health Sciences, Shanghai 201318, China
3. Publich Health College, Harbin Medical University, Harbin, 150086

*Correspondence address: Department of Inspection and Quarantine, Shanghai University of Medicine & Health Sciences, Shanghai, 279 Zhouzhu Rd, 201318, China.

Abstract

Background: Non-alcoholic fatty liver disease (NAFLD) is a clinical pathological syndrome characterized by excessive lipid deposition in hepatocytes, except alcohol and other definite liver damage factors. Emerging evidence indicates the involvement of long non-coding RNAs (LncRNAs) in regulating pathogenesis of NAFLD. However, the specific mechanism underlying this process still remains unclear.

Objective: The aim of this study was to investigate the functional implication of lncRNA Gm12664 in the hepatic lipid accumulation of NAFLD.

Methods: We applied the microarray approach to determine the differential expression profiles of lncRNAs, mRNAs and miRNAs in liver tissues of HFD-fed mice. Based on the co-expression networks between lncRNAs and lipogenesis-related genes during hepatic lipid accumulation in the pathogenesis of NAFLD, the role of LncRNA Gm12664 was further investigated and was focused on the regulation of CAV1. Besides, the miRNA microarray and bioinformatics analysis were used to predict the miRNA which might mediate the overexpression of CAV1 induced by Gm12664. *In vitro* and *in vivo* assays were performed to explore the biological effects of Gm12664 in hepatic lipid metabolism through the Gm12664/miR-295-5p/CAV1 axis.

Results: We found that lncRNA Gm12664 was markedly up-regulated and promoted CAV1 expression in both livers of HFD-fed mice and FFA-treated AML-12 cells. Suppression of

Gm12664 reversed FFA-induced triglyceride accumulation in AML-12 cells through down-regulation of CAV1. Further mechanistic studies demonstrated that miR-295-5p participated in the regulation of CAV1 by Gm12664 during hepatic lipid accumulation. Gm12664 positively regulated the expression of CAV1, through sponging mir-295-5p, and promoted hepatic lipid accumulation in the pathogenesis of NAFLD.

Conclusion: Our data are the first to document the working model of Gm12664 functions as a potential hepatocyte lipid accumulation facilitator. Gm12664 promotes hepatic lipid accumulation by binding to miR-295-5p, and eventually regulating the up-regulation of CAV1. Our results suggest the potency of Gm12664/miR-295-5p/CAV1 axis as a promising therapeutic target for NAFLD.

Keywords: non-alcoholic fatty liver disease; long non-coding RNA; Gm12664; miR-295-5p; CAV1; lipid accumulation

Introduction

Non-alcoholic fatty liver disease (NAFLD) is one of the most common causes of chronic liver disease, with the increased prevalence in the last few decades[1]. The histological spectrum of NAFLD ranged from simple steatosis to non-alcoholic steatohepatitis (NASH), which might led to cirrhosis and even hepatocellular carcinoma (HCC) eventually [2, 3]. The underlying mechanism for the development and progression of NAFLD is complex and multifactorial. Ectopic accumulation of triglyceride (TG), which is defined as hepatic TG accumulation above 5% of liver weight，occurs at the early stage and usually be regarded as the hallmark of NAFLD [4, 5]. Evidence has shown that triglyceride (TG) de novo lipogenesis is a prominent abnormality in NAFLD and the key event that leads to massive steatosis[5]. Some lipolytic enzymes, including hormone sensitive lipase (HSL) and triglyceride lipase (ATGL), and lipogenic enzymes, including fatty acid synthase (FAS) and diacylglycerol O-acyltransferase 2 (DGAT2) play vital roles in the regulation of triglyceride metabolism[6-8]. In addition, caveolin-1 (CAV1), a structural protein of caveolae, has been found to facilitate the efficient progression of liver regeneration and accumulation of triacylglycerols in hepatocytes [9-11]. Molecular details of regulating these lipid metabolism enzymes are needed to be figured out for developing potential therapeutic approaches for NAFLD.

Long non-coding RNAs (lncRNAs) are a class of transcripts with lengths greater than 200 nucleotides and act as guides, scaffolds, decoys and tethers of other biological molecules which are

involved in various biological processes [12-14]. In recent years, emerging evidence has revealed that LncRNAs act as important regulators during the pathophysiology of NAFLD[15-19]. Long noncoding RNA lncARSR was found to promote hepatic lipogenesis via Akt/SREBP-1c pathway and contribute to the pathogenesis of nonalcoholic steatohepatitis[18]. LncRNA SRA was reported to promote hepatic steatosis through repressing the expression of ATGL[19]. Despites the emerging studies focused on the function of lncRNAs during NAFLD, the exact role still remains largely unexplored. In our present study, lncRNA microarray analysis was performed to detect the expression of LncRNAs in liver tissues of HFD-induced mice, and we found that lncRNA Gm12664 level was significantly increased in both liver tissues of HFD-induced mice and FFA-treated AML-12 cells. The present study aimed to investigate the functional implication of Gm12664 in hepatocellular lipid metabolism and in the pathogenesis of NAFLD. Further study showed that Gm12664 promoted hepatocellular lipid accumulation through the upregulation of CAV1. By both *in vivo* and *in vitro* experiments, we further demonstrated that Gm12664 upregulates CAV1 expression by sponging miR-295-5p and contradicted the inhibitory effects of miR-295-5p on the CAV1 expression to promote lipid accumulation. These findings indicate that lncRNA Gm12664 functions as a competing endogenous RNA (ceRNA) for miR-295-5p to regulate CAV1 expression during excessive lipid deposition in the pathogenesis of NAFLD.

In conclusion, our study uncovers a new regulatory mechanism in the pathogenesis of hepatocellular lipid accumulation of NAFLD through the Gm12664/miR-295-5p/CAV1 axis, and provides new biomarkers for NAFLD and potential targets for therapeutic strategies and disease intervention (Figure 7).

Materials and Methods

Animals

Eight-week-old male C57BL/6 mice were purchased from Beijing Vital River Laboratory Animal Technology Co., Ltd. (Beijing, China). The animals were housed individually under a set temperature (18-22℃) and humidity(40-60%) with 12:12-h light/dark cycle, free access to standard laboratory food and water, and environmental noise kept to a minimum range. After 1 week adaptive feeding, the mice were treated for experiment. All animal experimental protocols were pre-approved by the Experimental Animal Ethic Committee Harbin Medical University.

Design one- Mice model of NAFLD

twenty mice were randomly divided into two groups and respectively fed a normal diet (NFD, 10% fat by energy) and a high-fat diet (HFD, 36% fat by energy) to establish a mice NAFLD model. The feeding experiment was continued for 10 weeks, during which daily food intake as well as weekly body weight were monitored. At the end of the 10th week, six mice were randomly picked from each group and were scanned with a Latheta LCT-200 (Hitachi, Japan) in a prone position to image the fat distribution. Body fat mass were calculated based on the scanned CT value. All mice were anesthetized by intraperitoneal injection with sodium pentobarbital (30mg/kg) and liver tissue samples were harvested stored at -80°C until use.

Design two- Lentivirus-mediated miR-295-5p knockdown in mice model

Another twenty mice were randomly divided into two groups and were injected intravenously through the tail vein with Amo-NC or Amo-miR295-5p lentivirus with PFU at 5×10^9 in 1 mL PBS. Amo-NC is the control lentivirus and Amo-miR295-5p is lentivirus of specific inhibition expression of miR-295-5p. A week later, the injection was repeated one time. The body weight of the mice were monitored weekly. Mice were sacrificed 10 weeks later after lentivirus injection and liver tissue samples were harvested stored at -80°C until use.

Cell experiments-cell culture，transfections and fluorescent microscopy

The mouse hepatocyte AML-12 cell line was used in this study. AML-12 cells were obtained from the American Type Culture Collection and were grown in DMEM/Ham's F12 media with 10% FBS mixed with 40-ng/mL dexamethasone and ITS. Cells were cultured at 37 °C in 5% CO2. To establish a cellular model of hepatic steatosis, AML-12 cells were treated for 24 h with stearic acid (SA, 300μmol/L) or palmitic acid (PA, 500μmol/L), respectively.

Lipofectamine 2000 (Invitrogen, Carlsbad, CA, USA) was used for transfection. SiRNA-Gm12664, siRNA-NC, mimics-NC, mimic-miR-295-5p, miR-295-5p inhibitor (Amo-miR295-5p) and inhibitor-NC (Amo-NC) were purchased from GenePharma (China) and, transfected into target cells using Lipofectamine 2000 (Invitrogen, Carlsbad, CA, USA) according to the manufacturer's instructions. The cell samples were then harvested for further analysis 48 h later after infection. At least three replicates of each experiment were performed.

BODIPY 493/503(4,4-difluoro-1,3,5,7-tetramethyl-4-bora3a,4a-diaza-s-indacene) is a fluorescent lipophilic stain widely used to label lipid droplets. Symbiodinium and purified LDs were stained with 38.2 mM BODIPY 493/503(Invitrogen, USA) in the dark for 20 min at RT. The stained cells

and LDs were visualized using the fluorescence microscope (Zeiss, Germany).

RNA extraction and microarray analysis of lncRNAs and mRNAs

Arraystar mouse lncRNA Microarray V2.0 designed for the global profiling of mouse lncRNAs and protein-coding transcripts was used for detecting lncRNAs and mRNAs. Total RNA was extracted using TRIzol reagent (Invitrogen, Shanghai, China) according to the manufacturer's instructions. RNA quantity and quality were measured by NanoDrop ND-1000, and RNA integrity was assessed by standard denaturing agarose gel electrophoresis. The RNA samples extracted (from liver tissue of NFD-fed and HFD-fed mice) were used to synthesized double-stranded cDNA and the RNA concentration (μg) to use in a reverse transcription reaction is 1ug/ul. The cDNA was then labeled and hybridized to the LncRNA Expression Microarray (Mouse LncRNA Microarray v2.0, Arraystar, USA) according to the manufacturer's protocol. After hybridization, the arrays were washed, and the slides were scanned with an Agilent Microarray Scanner (Agilent p/n G2565BA). Raw data were extracted as pair files using the Agilent Feature Extraction. The random variance model was used to identify the differentially expressed genes. The paired t-test was used to calculate the *P*-value. The threshold set for up and down-regulated genes was a fold change >=2.0 and a *P*-value <= 0.05, respectively. We have sent our data to Arrayexpress (https://www.ebi.ac.uk/fg/annotare/). lncRNA array data number is E-MTAB-8730, and miRNA array data number is E-MTAB-8731.

Real-time PCR analysis

Total RNA was isolated from the mouse liver tissues or AML-12 cells using TRIzol reagent (Invitrogen, Shanghai, China) according to the manufacturer's instructions. Reverse transcription reactions were performed using the PrimeScript RT reagent Kit (Takara, Tokyo, Japan) for mRNA detection. The primer sets used are listed in Supplemental Table 1. Quantitative real-time RT-PCR (qRT-PCR) analysis was performed using SYBR® Premix Ex TaqTM (Takara, Otus, Shiga, Japan). For detecting mature miR-295-5p, miRNAs were isolated from cells or liver tissues using the mirVana miRNA Isolation Kit (Ambion, Austin, TX, USA) according to the manufacturer's instructions. Reverse transcription and detection of miR-295-5p were carried out using NCode VILO miRNA cDNA Synthesis Kit and EXPRESS SYBR GreenER miRNA qRT-PCR Kit, respectively (Invitrogen, Carlsbad, CA, USA) according to the manufacturer's instructions. U6 was

used as an internal loading control. The SYBR green PCR Master Mix (Qiagen) was used for mRNA detection following the operating manual. The expression of Gapdh as an endogenous control. The resulting cDNA was quantified with the ABI 7500 FAST real-time PCR System (Applied Biosystems, Carlsbad, USA). Levels of relative expression were calculated and quantified with the $2^{-\Delta\Delta Ct}$ method after normalization with the expression level of endogenous control.

Triglyceride Assay

Intrahepatic and intracellular triglyceride (TG) level was quantified using commercial kits (E1013, E1015; Applygen Technologies Inc., Beijing, China) according to the manufacturer's instructions. Briefly, collected liver tissue homogenates or cells were treated with lysis buffer on ice. Lysates were heated at 70˚C for 10 min, and centrifuged at 2000 rpm for 5 min at room temperature. The supernatant was then assessed with according working solution. TG value was normalized with the total protein levels. The protein concentration in the resulting lysates was determined using the bicinchoninic acid protein assay kit (Applygen Technologies Inc.).

Dual luciferase reporter assay

The 3'UTR of mice CAV1 (NM_007616, 2542 bp bp, GenBank) was amplified via PCR using the genomic DNA of mice liver tissues. Then, the PCR fragment was inserted into the psiCHECK-2 vector (Promega, Madison, WI, USA) with the In-fusion Advantage PCR Cloning Kit (Clontech, Mountain View, CA, USA). HEK-293T were co-transfected with the CAV1 3'-UTR and miR-295-5p mimics (GenePharma, Shanghai, China). After 48 h, the luciferase activity was analyzed using the Dual-Luciferase Reporter Assay System (Promega) according to the manufacturer's protocol. Three independent co-transfection experiments were carried out. The firefly luciferase activity of each transfected well was normalized to renilla luciferase activity.

Western blotting analyses

In brief, mouse liver tissue and cells were homogenized by RIPA lysis buffer (150 mM Tris-HCl, 50 mM NaCl, 1% NP-40, 0.1% tween- 20), and centrifuged at 15,000 g for 15 min. Then, the supernatant was mixed with loading buffer [125 mM Tris hydrochloride (pH 6.8), 10% mercaptoethanol (vol/vol), 4% SDS (wt/vol), 20% glycerol (vol/vol), and 0.002% bromophenol blue] and then was heated at 100 °C for 10 min. Supernatants were subjected to 10% SDS-PAGE

gels. the membranes were incubated at 4°C overnight with the following primary antibodies: anti-β-actin (1:800, 4970, Cell Signaling Technology, Danvers, USA), anti- CAV1 (1:1000, 3267, Cell Signaling Technology, Danvers, USA), anti- ATGL (1:1000, 2439, Cell Signaling Technology, Danvers, USA), anti- HSL (1:10000, 18381，Cell Signaling Technology, Danvers, USA), anti-DGAT2(1:1000, sc-293211, Santa Cruz Biotechnologies, CA, USA) and anti- FAS (1:10000, 4233, Cell Signaling Technology, Danvers, USA). After 3 washes, the membrane was incubated with horseradish peroxidase (HRP)-coupled secondary antibodies for 1 h at room temperature. The membrane was washed again, and the proteins were visualized with an enhanced chemiluminescence (ECL) kit (Millipore, Billerica, MA, USA). Band intensities were measured by Image. J software and normalized to β-actin. Data were represented as mean ± SD of three independent experiments.

Histological Analysis

Haematoxylin-eosin (HE) staining was performed to examine liver tissue morphology following standard protocols. In brief, the live tissues were fixed intra-tracheally with 4% paraformaldehyde in phosphate buffer and were embedded in paraffin. Sections (4 μm) were stained with haematoxylin (5%) for 10 min. Tissue slices were first rinsed in distilled water, acidified and then stained in eosin for 5 min. After dehydration and coverslip mounting, tissue slices were observed under a bright field microscope.

Statistical analyses

Experimental data are processed with SPSS17.0 statistical software and presented as the average (mean ± SD) of results from at least three separate experiments. Student's t-test was used for statistical comparison between two groups. The above data with more than two groups were analyzed with one-way ANOVA. P-values<0.05 were considered statistically different.

Results

The establishment of high-fat diet induced mice model for NAFLD mechanism research

We confirmed the HFD mice model was made successfully before deprivation of liver tissue. In records, the body weight of HFD mice were visibly increased from day 21 when compared with that in control mice (Figure 1A). In addition, compared with controls, increased body fat percentage in

HFD fed mice was observed at the end of 10th week (Figure 1B). Compared with those in control mice, the protein expression of endogenous lipogenic enzymes, FAS and DGAT2, was up-regulated in liver samples of HFD-fed mice, while the expression of lipolytic enzymes, HSL and ATGL, was down-regulated (Figure 1C). In addition, liver CAV1 protein expression of HFD-induced mice exhibited increased (Figure 1C). These data indicated the successful development of the HFD-induced mice model for NAFLD.

LncRNA Gm12664 was up-regulated in livers of HFD-fed mice and FFA-treated hepatocytes

Herein, we aimed to acquire expression profiles of lncRNAs and messenger RNAs (mRNAs) in HFD-fed mice model of NAFLD to identify the deregulated lncRNAs under this pathological setting. In lncRNA microarray analyses, we identified 751 differentially expressed lncRNAs, including 364 up-regulated and 387 down-regulated lncRNAs in HFD-fed mice, compared with those in control mice (Figure 2A). Compared with the control group, there were 434 up-regulated and 394 down-regulated mRNAs that showed differential expression after HFD-fed (Figure 2B). To determine the potential interaction between differentially-expressed lncRNAs and mRNAs during hepatic lipid metabolism, the coding-non-coding gene (CNC) co-expression network was constructed based on the correlation analysis via computational prediction algorithms. Intriguingly, 19 lncRNAs were found to be highly correlated with the expression of mRNAs (Figure 2C and Supplement Table 2). We picked 15 lncRNAs at random from 19 lncRNAs to verify the lncRNA microarray by the RT-qPCR. The results showed that, 15 lncRNAs exhibited the same expression patterns as the microarray data (Figure 2D). Among these lncRNAs, Gm12664 caught our attention because of its highly and positively correlated with the expression of CAV1, known as an important factor in the development of NAFLD by promoting lipid accumulation [10, 11]. As shown in Figure 2E and 2F, Gm12664 expression was significantly increased in both HFD-fed mice liver tissues and AML-12 cells treated with PA or SA. These results indicated that Gm12664 may play an important role in the pathological process of hepatic lipid metabolism. Previously, Gm12664 function in lipid metabolism has still not been reported, so we selected Gm12664 for further experimental investigations.

The inhibition of Gm12664 expression reduced triglyceride accumulation in AML-12 cells through down-regulation of CAV1

To explore whether the inhibition of Gm12664 affects triglyceride accumulation, we transfected siRNA-Gm12664 into AML-12 cells to markedly suppress Gm12664 expression (Figure 3A). Then, we checked if the inhibition of Gm12664 affects the expression of the key enzymes of triglyceride metabolism. As shown in Figure 3B, the levels of FAS, DGAT2, HSL and ATGL showed no significant difference compared with control group. However, siRNA-Gm12664 significantly reduce the mRNA and protein level of CAV1 (Figure 3C and 3D). Combined with the microarray data analysis, these results suggested that Gm12664 promoted triglyceride accumulation through up-regulation of CAV1 in the pathogenesis of NAFLD.

LncRNA Gm12664 was physically associated with miR-295-5p in the process of lipid metabolism

Next, we explored the potential mechanism by which Gm12664 regulates CAV1 expression. It is well known that lncRNAs can function as ceRNAs to protect mRNAs by competing for their targeting microRNAs. Therefore, we investigated whether Gm12664 played such a role. The miRNA microarray analysises was performed to explore the expression profiles of miRNAs using the same liver tissues of HFD-fed mice as above lncRNA microarray (Figure 4A). KEGG and Mirpath signaling pathway analyses were performed to annotate miRNAs related to triglyceride metabolism. A total of 6 most relevant miRNAs were identified, including miR-295-5p, miR-183-5p, miR-125a-3p, miR-222-3p, miR-881-5p and miR-155-3p. To further explore which miRNAs that Gm12664 could directly regulate, we investigated these six miRNAs expression using siRNA-Gm12664 AML-12 cell model. As illustrated in Figure 4B, only the amount of miR-295-5p significantly increased after Gm12664 inhibition. Strikingly, the expression level of miR-295-5p was markedly reduced in HFD-fed mice liver tissues (Figure 4C). These results suggested that Gm12664 was physically associated with miR-295-5p in the process of lipid metabolism. Moreover, using bioinformatics (DianaTools, miRcode Starbase v2.0 and RNAhybrid), we found that miR-295-5p has putative binding sites with Gm12664 (Figure 4D).

To determine whether the expression of miR-295-5p was regulated by Gm12664, two sets of studies were carried out. First, we examined the change of miR-295-5p expression level in AML-12 cells with SA and PA intervention. Strikingly, raising Gm12664 level by SA and PA treatment stimulated the down-regulation of miR-295-5p expression level (Figure 4E). Subsequently, we determined if inhibiting Gm12664 expression using siRNA-Gm12664 could affect miR-295-5p

level. As shown in Figure 4F and 4G, the inhibition of Gm12664 expression down-regulated miR-295-5p. Both *in vivo* and *in vitro* results suggested an inverse correlation between Gm12664 and miR-295-5p expression levels, which supported that miR-295-5p is a Gm12664-targeting miRNA.

miR-295-5p down-regulates CAV1 expression

We predicted the target genes of miR-295-5p using bioinformatics databases (DianaTools, miRcode Starbase v2.0 and RNAhybrid) and were surprised to find that CAV1 was predicted to be a direct target of miR-295-5p (Figure 5A). To further investigate the correlation between miR-295-5p and CAV1, we constructed luciferase reporters containing the wild-type CAV1 3'-UTR. Our results indicate that miR-295-5p mimic significantly reduced the luciferase reporter activities of the wild-type CAV1 reporter compared to the control, suggesting that CAV1 was physically associated with miR-295-5p via these sites (Figure 5B). Correspondingly, overexpression of miR-295-5p caused significant decrease of both RNA and protein levels of CAV1 in AML-12 cells (Figure 5C). In order to verify the regulation of CAV1 by miR-295-5p *in vivo*, we inhibited the expression of miR-295-5p in C57/BL mice by tail vein injection of lentivirus. The antagomir lentivirus of miR-295-5p (Amo-miR-295-5p) efficiently attenuated the miR-295-5p levels *in vivo* (Supplemental Figure 1). As expected, after the down-regulation of miR-295-5p, the expression levels of CAV1 protein in liver tissues were significantly higher compared to the control (Figure 5D). Taken together, these results indicated that CAV1 is a direct miR-295-5p target.

The inhibition of miR-295-5p increased lipid accumulation in hepatocytes and C57/BL mice

We further identified the functional role of miR-295-5p in lipid accumulation. As shown in Figure 6A and 6B, down-regulation of miR-295-5p significantly promoted the intracellular lipid accumulation in AML-12 cells. After the injection of lentivirus, there had no significant difference in body weight between the two groups. However, the body fat rate of the mice in miR-295-5p inhibition group was significantly higher than that in the control group (Figure 6C). Moreover, miR-295-5p knockdown *in vivo* resulted in a significant increase in triglyceride content in the liver (Figure 6D). Histopathological examination revealed a significant lipid accumulation in the liver tissue of miR-295-5p inhibition group (Figure 6E). These data indicated that miR-295-5p inhibits lipid accumulation in hepatocytes.

Taken together these results indicate that lncRNA Gm12664 sponges mir-295-5p to positively regulate CAV1 expression, which promotes hepatic lipid accumulation (Figure 7).

Discussion

In the present study, we first identified a novel role of Gm12664 in promoting hepatocellular lipid accumulation, which are important in the pathogenesis of NAFLD. We found that lncRNA Gm12664 was markedly up-regulated in both livers of HFD-fed mice and FFA-treated AML2 cells. Suppression of Gm12664 expression decreased FFA-induced triglyceride accumulation in AML2 cells through down-regulation of CAV1, the key regulatory molecule involved in lipogenesis. Further mechanistic studies indicated that miR-295-5p participated in the regulation of CAV1 by Gm12664. We demonstrated that Gm12664 inhibited miR-295-5p expression, which further up-regulated CAV1 expression, eventually promoting hepatocellular lipid accumulation. This newly identified Gm12664/miR-295-5p/CAV1 regulatory axis provides a novel clue to the pathogenesis of NAFLD.

Emerging evidence has revealed that LncRNAs function as important contributors to biological processes underlying the pathophysiology of NAFLD[18-20]. For instance, lncRNA MEG3 regulated hepatic lipid mechanism through AKT-mTOR signalling pathway[20]. Long noncoding RNA lncARSR was found to promote hepatic lipogenesis via Akt/SREBP-1c pathway and contribute to the pathogenesis of nonalcoholic steatohepatitis[18]. LncRNA SRA was reported to promote hepatic steatosis through repressing the expression of ATGL[19]. However, the panoramic view on what and how lncRNAs contribute to the pathophysiology of NAFLD is still largely unclear. In the present study, we found that LncRNA Gm12664 level was significantly increased in liver tissues of HFD-fed mice based on the microarray analysises. LncRNA Gm12664 is located in the antisense strand of mouse chromosome 11 at 1653411-1664911, and its length was 913bp. Currently, no other study has reported the role of lncRNA Gm12664 in NAFLD. Here, we demonstrated that lncRNA Gm12664 expression remarkably up-regulated in both the liver of HFD-induced mice and FFA-treated AML-12 cells. Moreover, Gm12664 down-regulation suppressed TG accumulation, providing direct evidence for the important role of Gm12664 in the pathological process of NAFLD.

Fatty acid and fat synthesis in the liver is a highly regulated metabolic pathway, and several lipogenic genes are simultaneously regulated at the transcription level[6-8]. The lipolytic enzymes

(HSL and ATGL) and lipogenic enzymes (FAS and DGAT2) are well acknowledged to act as vital roles in the regulation of triglyceride metabolism. In addition, emerging evidence has shown that CAV1, the structural protein of caveolar in the plasma membrane, is required for hepatic lipid accumulation, lipid and glucose metabolism, mitochondrial biology, and hepatocyte proliferation[9, 21-24]. CAV1-deficient mice lack the ability to store triglycerides in adipose tissue, to resist obesity induced by high-fat diet, and to reduce the formation of lipid droplets in liver cells[9, 25, 26]. In our study, endogenous lipogenic enzymes (FAS and DGAT2) and CAV1 protein were significantly up-regulated, and lipolytic enzymes (HSL and ATGL) were down-regulated in liver samples of HFD-fed mice, which is consistently in agreement with the results of literatures. CAV1 caught our attention because CAV1 expression was highly correlated with Gm12664, based on the CNC co-expression analysis of microarray results. The down-regulation of Gm12664 significantly decreased TG accumulation and CAV1 expression, but FAS, DGAT2, HSL and ATGL expression showed no significant difference, compared with control group. These results provide indirect evidence that Gm12664 probably regulated liver lipid accumulation by CAV1.

Many current studies have showed that lncRNAs regulate gene expression indirectly via transcriptional regulation, posttranscriptional modification, and modulation of microRNA (miRNA) activities[21, 27, 28]. Among them, the most common mechanism is that lncRNAs can function as competing endogenous RNAs (ceRNAs) to protect mRNAs by competing for their targeting microRNAs[19, 20]. Hence, we hypothesized that Gm12664 played such a role in regulation CAV1. In follow-up experiments, we identified 7 differentially expressed miRNAs that may be associated with regulating lipid mechanism, based on miRNA microarray analysis and bioinformatics databases. Among these 7 miRNAs, only miR-295-5p was notably reduced in Gm12664 over-expressing cells. And Gm12664 silencing significantly increased the expression of miR-295-5p in AML-12 cells. Moreover, miR-295-5p knockdown in C57/BL mice and AML-12 cells increased lipid accumulation, which indicated miR-295-5p is a Gm12664-targeting miRNA in hepatocellular lipid accumulation.

Further mechanistic studies indicated that miR-295-5p participated in the regulation of hepatocellular lipid accumulation by CAV1. Our study is the first report to identify the binding affinity between miR-295-5p and the 3'UTR of CAV1 gene transcripts in AML-12 cells validated by luciferase activity assay. Consistent with the observations from miR-295-5p overexpression, knockdown of mir-295-5p significantly increased CAV1 expression *in vivo* and *in vitro*. Based on

these data, we demonstrated that CAV1 is a target of miR-295-5p. For further examining the functional role of miR-295-5p in regulating CAV1 expression and lipid accumulation, we established lentivirus-mediated miR-295-5p knockdown mice model. As shown in our results, CAV1 expression and triglyceride accumulation in the liver of miR-295-5p knockdown mice model was significanltly increased, indicated that miR-295-5p playe a role in hepatocellular lipid accumulation through regulating CAV1.

In summary, our study reveals a novel and important role of lncRNA Gm12664 regulating hepatocellular lipid accumulation via Gm12664/miR-295-5p/CAV1 regulatory axis for the first time. FFAs promoted Gm12664 expression down-regulating miR-295-5p, which further up-regulates CAV1 expression, eventually leading to hepatocellular lipid accumulation. These results collectively suggested the potency of Gm12664 as an early biomarker for NAFLD and as a drug target for disease intervention.

Financial interests

All authors report no conflicts of interest

Acknowledgment

This work was supported by the National Natural Science Foundation of China (number 81202188) and the Produce-Learn-Research Projects of Shanghai University of Medicine & Health Sciences (number B1-0200-19-311144). The funders had no role in study design, data collection and interpretation, or the decision to submit the work for publication.

Author contributions

Lixin Na and Fei Xu conceived and designed the study. Fei Xu, Zhenfeng Song and Linjun Chen performed the experiments. Liqiang Wang and Qingwen Zhang participated in the data collection and analysis. Fei Xu and Lixin Na interpreted the data and wrote the manuscript. All authors read and approved the final manuscript.

Conflicts of interest

The authors declare no conflicts of interest

References

1. Ong JP, Younossi ZM: Epidemiology and natural history of NAFLD and NASH. *Clinics in liver disease* 2007, 11(1):1-16, vii. https://doi.org/10.1016/j.cld.2007.02.009
2. Takakura K, Koido S, Fujii M, Hashiguchi T, Shibazaki Y, Yoneyama H, Katagi H, Kajihara M, Misawa T, Homma S *et al*: Characterization of non-alcoholic steatohepatitis-derived hepatocellular carcinoma as a human stratification model in mice. *Anticancer research* 2014, 34(9):4849-4855. https://doi.org/10.1245/s10434-014-3557-1
3. Guerrero R, Vega GL, Grundy SM, Browning JD: Ethnic differences in hepatic steatosis: an insulin resistance paradox? *Hepatology* 2009, 49(3):791-801. https://doi.org/10.1002/hep.22726
4. Korenblat KM, Fabbrini E, Mohammed BS, Klein S: Liver, muscle, and adipose tissue insulin action is directly related to intrahepatic triglyceride content in obese subjects. *Gastroenterology* 2008, 134(5):1369-1375. https://doi.org/10.1053/j.gastro.2008.01.075
5. Lambert JE, Ramos-Roman MA, Browning JD, Parks EJ: Increased de novo lipogenesis is a distinct characteristic of individuals with nonalcoholic fatty liver disease. *Gastroenterology* 2014, 146(3):726-735. https://doi.org/10.1053/j.gastro.2013.11.049
6. Hoang NA, Richter F, Schubert M, Lorkowski S, Klotz LO, Steinbrenner H: Differential capability of metabolic substrates to promote hepatocellular lipid accumulation. *European journal of nutrition* 2018. https://doi.org/10.1007/s00394-018-1847-2
7. Honma M, Sawada S, Ueno Y, Murakami K, Yamada T, Gao J, Kodama S, Izumi T, Takahashi K, Tsukita S *et al*: Selective insulin resistance with differential expressions of IRS-1 and IRS-2 in human NAFLD livers. *International journal of obesity* 2018, 42(9):1544-1555. https://doi.org/10.1038/s41366-018-0062-9
8. Schenkel LC, Sivanesan S, Zhang J, Wuyts B, Taylor A, Verbrugghe A, Bakovic M: Choline supplementation restores substrate balance and alleviates complications of Pcyt2 deficiency. *The Journal of nutritional biochemistry* 2015, 26(11):1221-1234. https://doi.org/10.1016/j.jnutbio.2015.05.014
9. Fernandez-Rojo MA, Gongora M, Fitzsimmons RL, Martel N, Martin SD, Nixon SJ, Brooks AJ, Ikonomopoulou MP, Martin S, Lo HP *et al*: Caveolin-1 is necessary for hepatic oxidative lipid metabolism: evidence for crosstalk between caveolin-1 and bile acid signaling. *Cell reports* 2013, 4(2):238-247. https://doi.org/10.1016/j.celrep.2013.06.017
10. Fernandez-Rojo MA, Ramm GA: Caveolin-1 Function in Liver Physiology and Disease. *Trends in molecular medicine* 2016, 22(10):889-904. https://doi.org/10.1016/j.molmed.2016.08.007
11. Fernandez-Rojo MA, Restall C, Ferguson C, Martel N, Martin S, Bosch M, Kassan A, Leong GM, Martin SD, McGee SL *et al*: Caveolin-1 orchestrates the balance between glucose and lipid-dependent energy metabolism: implications for liver regeneration. *Hepatology* 2012, 55(5):1574-1584. https://doi.org/10.1002/hep.24810
12. Rinn JL, Chang HY: Genome regulation by long noncoding RNAs. *Annual review of biochemistry* 2012, 81:145-166. https://doi.org/10.1146/annurev-biochem-051410-092902
13. Tsai MC, Manor O, Wan Y, Mosammaparast N, Wang JK, Lan F, Shi Y, Segal E, Chang HY: Long noncoding RNA as modular scaffold of histone modification complexes. *Science* 2010, 329(5992):689-693. https://doi.org/10.1126/science.1192002
14. Wang KC, Yang YW, Liu B, Sanyal A, Corces-Zimmerman R, Chen Y, Lajoie BR, Protacio A, Flynn RA, Gupta RA *et al*: A long noncoding RNA maintains active chromatin to coordinate homeotic gene expression. *Nature* 2011, 472(7341):120-124.

https://doi.org/10.1038/nature09819
15. Zhao XY, Xiong X, Liu T, Mi L, Peng X, Rui C, Guo L, Li S, Li X, Lin JD: Long noncoding RNA licensing of obesity-linked hepatic lipogenesis and NAFLD pathogenesis. *Nature communications* 2018, 9(1):2986. https://doi.org/10.1038/s41467-018-05383-2
16. Atanasovska B, Rensen SS, van der Sijde MR, Marsman G, Kumar V, Jonkers I, Withoff S, Shiri-Sverdlov R, Greve JWM, Faber KN *et al*: A liver-specific long noncoding RNA with a role in cell viability is elevated in human nonalcoholic steatohepatitis. *Hepatology* 2017, 66(3):794-808. https://doi.org/10.1002/hep.29034
17. Zhang M, Chi X, Qu N, Wang C: Long noncoding RNA lncARSR promotes hepatic lipogenesis via Akt/SREBP-1c pathway and contributes to the pathogenesis of nonalcoholic steatohepatitis. *Biochemical and biophysical research communications* 2018, 499(1):66-70. https://doi.org/10.1016/j.bbrc.2018.03.127
18. Li Y, Ye Y, Feng B, Qi Y: Long Noncoding RNA lncARSR Promotes Doxorubicin Resistance in Hepatocellular Carcinoma via Modulating PTEN-PI3K/Akt Pathway. *Journal of cellular biochemistry* 2017, 118(12):4498-4507. https://doi.org/10.1002/jcb.26107
19. Chen G, Yu D, Nian X, Liu J, Koenig RJ, Xu B, Sheng L: LncRNA SRA promotes hepatic steatosis through repressing the expression of adipose triglyceride lipase (ATGL). *Scientific reports* 2016, 6:35531. https://doi.org/10.1038/srep35531
20. Huang P, Huang FZ, Liu HZ, Zhang TY, Yang MS, Sun CZ: LncRNA MEG3 functions as a ceRNA in regulating hepatic lipogenesis by competitively binding to miR-21 with LRP6. *Metabolism: clinical and experimental* 2019, 94:1-8. https://doi.org/10.1016/j.metabol.2019.01.018
21. Ebert MS, Neilson JR, Sharp PA: MicroRNA sponges: competitive inhibitors of small RNAs in mammalian cells. *Nature methods* 2007, 4(9):721-726. https://doi.org/10.1038/nmeth1079
22. Watanabe M, Houten SM, Wang L, Moschetta A, Mangelsdorf DJ, Heyman RA, Moore DD, Auwerx J: Bile acids lower triglyceride levels via a pathway involving FXR, SHP, and SREBP-1c. *The Journal of clinical investigation* 2004, 113(10):1408-1418. https://doi.org/10.1172/JCI21025
23. Stremmel W, Staffer S, Wannhoff A, Pathil A, Chamulitrat W: Plasma membrane phospholipase A2 controls hepatocellular fatty acid uptake and is responsive to pharmacological modulation: implications for nonalcoholic steatohepatitis. *FASEB journal : official publication of the Federation of American Societies for Experimental Biology* 2014, 28(7):3159-3170. https://doi.org/10.1096/fj.14-249763
24. Qiu Y, Liu S, Chen HT, Yu CH, Teng XD, Yao HT, Xu GQ: Upregulation of caveolin-1 and SR-B1 in mice with non-alcoholic fatty liver disease. *Hepatobiliary & pancreatic diseases international : HBPD INT* 2013, 12(6):630-636.
25. Cohen AW, Schubert W, Brasaemle DL, Scherer PE, Lisanti MP: Caveolin-1 expression is essential for proper nonshivering thermogenesis in brown adipose tissue. *Diabetes* 2005, 54(3):679-686. https://doi.org/10.2337/diabetes.54.3.679
26. Razani B, Combs TP, Wang XB, Frank PG, Park DS, Russell RG, Li M, Tang B, Jelicks LA, Scherer PE *et al*: Caveolin-1-deficient mice are lean, resistant to diet-induced obesity, and show hypertriglyceridemia with adipocyte abnormalities. *The Journal of biological chemistry* 2002, 277(10):8635-8647. https://doi.org/10.1074/jbc.M110970200
27. Zhu J, Yu W, Wang Y, Xia K, Huang Y, Xu A, Chen Q, Liu B, Tao H, Li F *et al*: lncRNAs: function and mechanism in cartilage development, degeneration, and regeneration. *Stem cell research & therapy* 2019, 10(1):344. https://doi.org/10.1186/s13287-019-1458-8

28. Zhou Q, Yu Q, Gong Y, Liu Z, Xu H, Wang Y, Shi Y: Construction of a lncRNA-miRNA-mRNA network to determine the regulatory roles of lncRNAs in psoriasis. *Experimental and therapeutic medicine* 2019, 18(5):4011-4021. https://doi.org/10.3892/etm.2019.8035

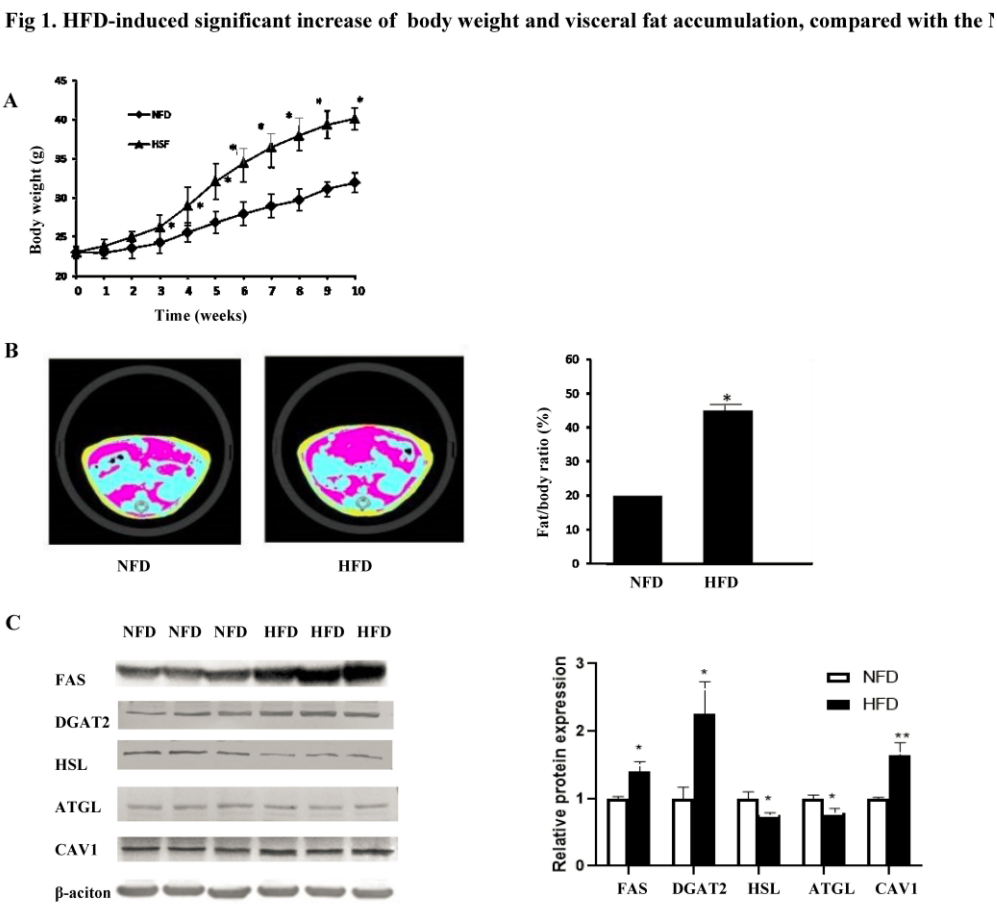

Fig 1. HFD-induced significant increase of body weight and visceral fat accumulation, compared with the NFD group.

(A) The feeding experiment in C57/BL mice was continued for 10 weeks, during which weekly body weights was monitored weekly. Eight-week feeding with the HFD resulted in significant increase in body weight.

(B) CT images of body fat distribution showed the richer subcutaneous and visceral fat were in the HFD group , compared with the NFD group. The ratio of fat to body weight in HFD-fed group and the control group was computed as fat mass/total body weight × 100%.

(C) Representative western blots for FAS, DGAT2, HSL, ATGL and CAV1 expression in the liver tissue of the control group and the high-fat group. β-actin was used for normalization.

Values are means ± SD of data from three separate experiments. *P < 0.05 compared with controls.

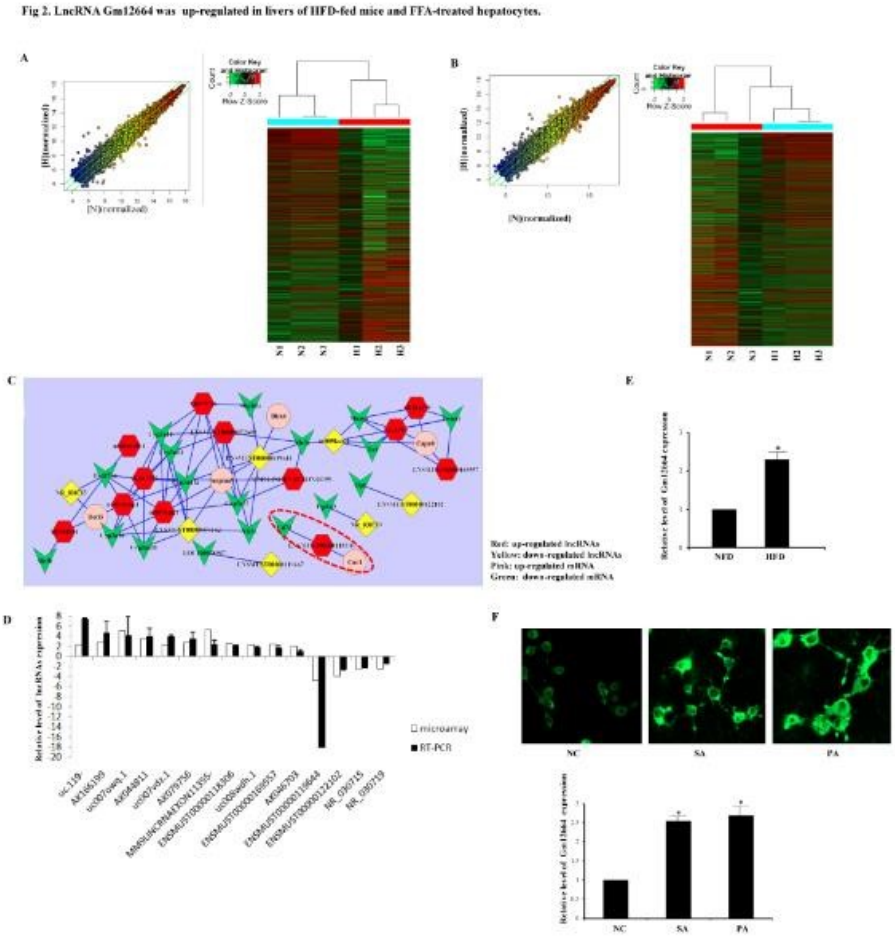

Fig 2. LncRNA Gm12664 was up-regulated in livers of HFD-fed mice and FFA-treated AML-12 cells.

(A) Scatter plot (left), heat map depiction of LncRNAs (right) differentially expressed in the liver of HFD mice as examined by LncRNAs microarray. N1 N2 N3: the control groups. H1 H2 H3: the high-fat groups.

(B) Scatter plot (left), heat map depiction of mRNAs (right) differentially expressed in the liver of HFD mice as examined by mRNAs microarray. N1 N2 N3: the control groups. H1 H2 H3: the high-fat groups.

(C) The co-expression networks of the lncRNAs and mRNAs were constructed using Cytoscape software. The up-regulated lncRNAs are shown by the red rectangle. The yellow rectangles represent the down-regulated lncRNAs. The up-regulated mRNAs are shown by the pink rectangle. The green rectangles represent the down-regulated mRNAs.

(D) Differential expression analysis of lncRNAs (>2-fold down or up) observed in results described in A and C. Microarray is the result of lncRNAs microarray. RT-PCR is the result of real-time PCR.

(E) Levels of lncRNA Gm12664 in the liver tissue of the control group and the high-fat group as measured by RT-PCR analysis.

(F) PA and SA increased Gm12664 expression in AML-12 cells. CN: control group. SA: stearic acid group. PA: palmitic acid group. (SA 300μmol/L and PA 500μmol/L)

Up: Bodipy 493/503 staining was used to observe the morphology and amount of intracellular lipid droplets under fluorescence microscope.

Down: The level of lncRNA Gm12664 expression was measured by RT-PCR analysis.

All the values are means ± SD of data from three separate experiments . *$P < 0.05$ compared with controls.

Fig 3. Inhibition of Gm12664 expression reduces triglyceride accumulation in AML-12 cells through down-regulation of CAV1.

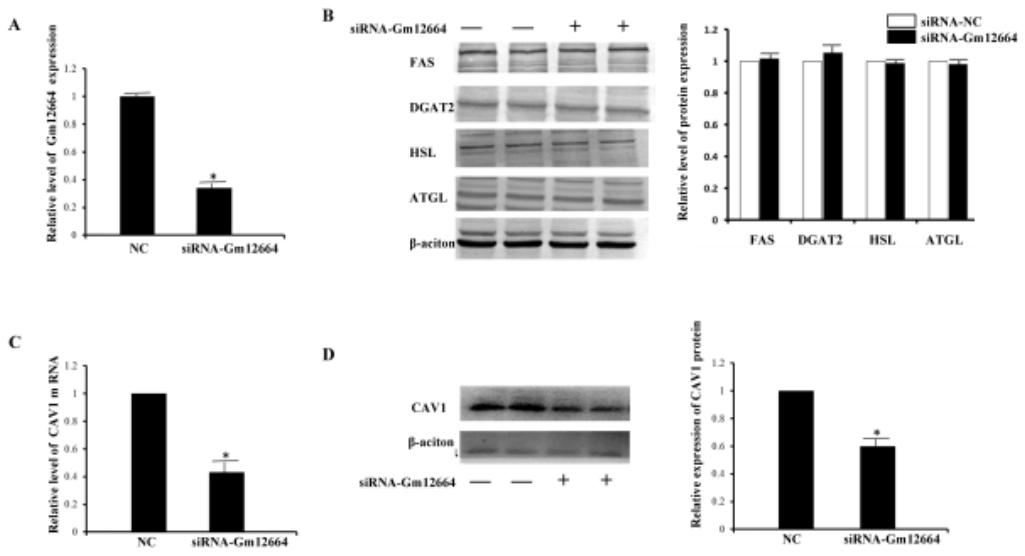

Fig 3. Inhibition of Gm12664 expression reduces triglyceride accumulation in AML-12 cells through down-regulation of CAV1.

(A) The expression level of Gm12664 in AML-12 cell transfected with siRNA-Gm12664 for 48 as measured by RT-PCR.

(B) Representative western blots and the quantification for FAS, DGAT2, HSL and ATGL expression in 48 h after transfection with siRNA-NC or siRNA-Gm12664 in AML-12 cells. β-actin was used for normalization.

(C) The expression levels of CAV1 mRNA were evaluated by qRT-PCR in AML-12 cell transfected with siRNA-Gm12664 for 48h.

(D) The expression levels of CAV1 protein were evaluated by western blot in AML-12 cell transfected with siRNA-Gm12664 for 48h.

All the values are means ± SD from three separate experiments. *$P < 0.05$ compared with controls.

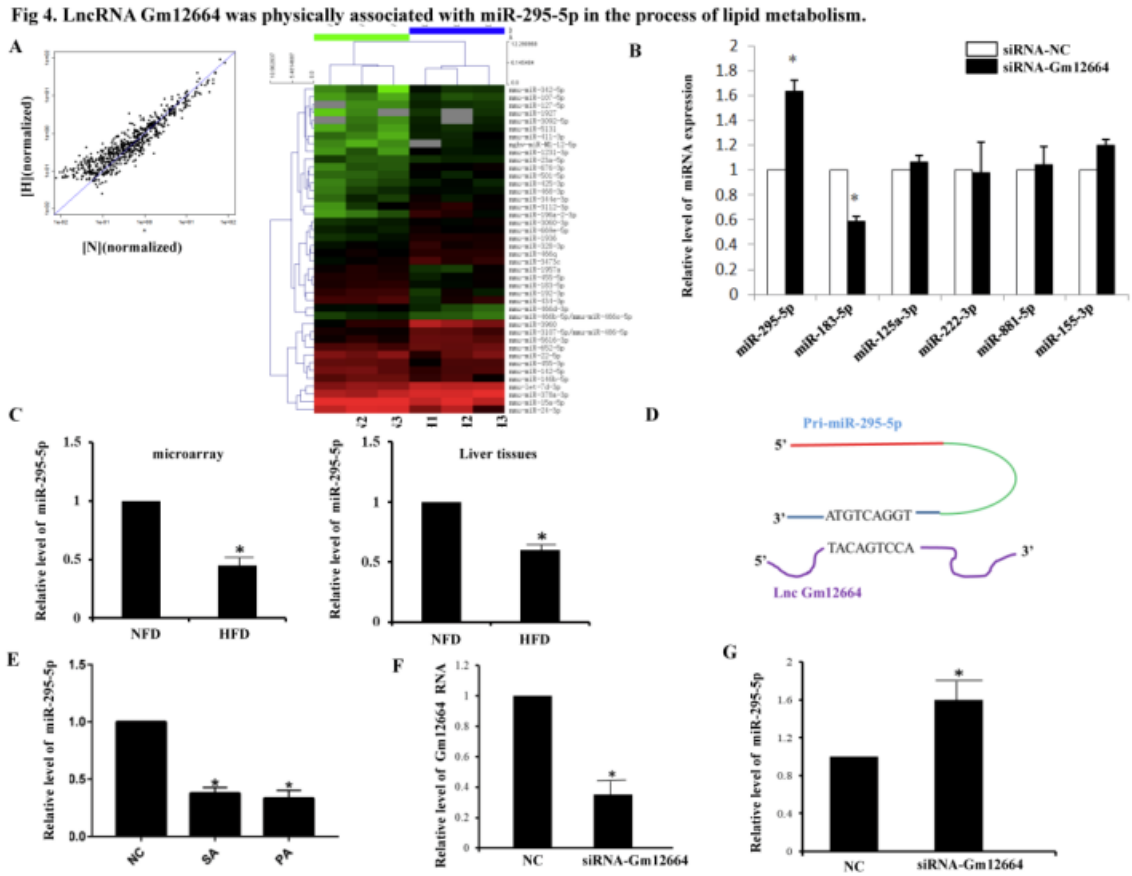

Fig 4. LncRNA Gm12664 was physically associated with miR-295-5p in the process of lipid metabolism.

(A) Scatter plot (left), heat map depiction (middle) and volcano plots of miRNAs differentially expressed in the liver of HFD mice as examined by miRNAs microarray.

(B) Levels of miR-295-5p, miR-183-5p, miR-125a-3p, miR-222-3p, miR-881-5p and miR-155-3p in AML-12 cells were transfected with siRNA-NC or siRNA-Gm12664 for 48h as measured by RT-PCR analysis.

(C) Levels of miR-295-5p using miRNAs microarray samples and the liver tissue samlpes of NFD mice and HFD-mice as measured by RT-PCR analysis.

(D) Schematic of miR-295-5p depicting the stem-loop sequence and its complementarity with lncRNA Gm12664 predicted by bioinformatics.

(E) PA and SA decreased miR-295-5p expression in AML-12 cells. The level of miR-295-5p expression was measured by RT-PCR analysis. CN: control group. SA: stearic acid group. PA: palmitic acid group.

(F) The expression level of Gm12664 in AML-12 cell transfected with siRNA-Gm12664 for 48 as measured by RT-PCR.

(G) The expression level of miR-295-5p in AML-12 cell transfected with siRNA-Gm12664 for 48 as measured by RT-PCR.

All the values are means ± SD from three separate experiments. *P < 0.05 compared with controls.

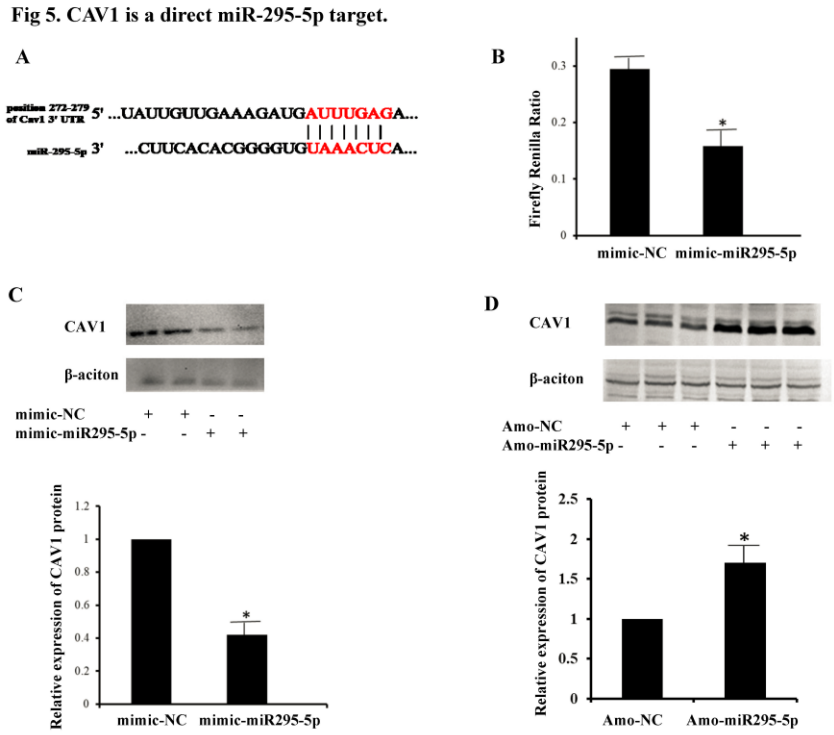

Fig 5. CAV1 is a direct miR-295-5p target.

(A) Bioinformatics predicted miR-295-5p binding sites in CAV1. Partial sequences of miR-295-5p and binding sites in the CAV1 3'UTR are shown. .

(B) Luciferase assay. HEK293T cells were infected with adenoviral miR-295-5p or β-gal, then transfected with the luciferase constructs of Luc-CAV1-3'UTR. The luciferase activity was analysed.

(C) Representative western blots and quantification PCR of CAV1 protein level in AML-12 cells transfected for 48h with mimic-NC or mimic-miR-295-5p for 48h. β-actin was used for normalization.

(D) Knockdown of miR-295-5p increased CAV1 level in liver and in adipose tissues. Representative western blots and the quantification PCR for CAV1 expression in the liver of C57/BL mice injected into the veins of the tails Amo-NC or Amo-miR295-5p lentivirus. β-actin was used for normalization. Amo-NC is control group, and Amo-miR295-5p is inhibition of miR-295-5p expression group.

All the values are means ± SD from three separate experiments. *$P < 0.05$ compared with controls.

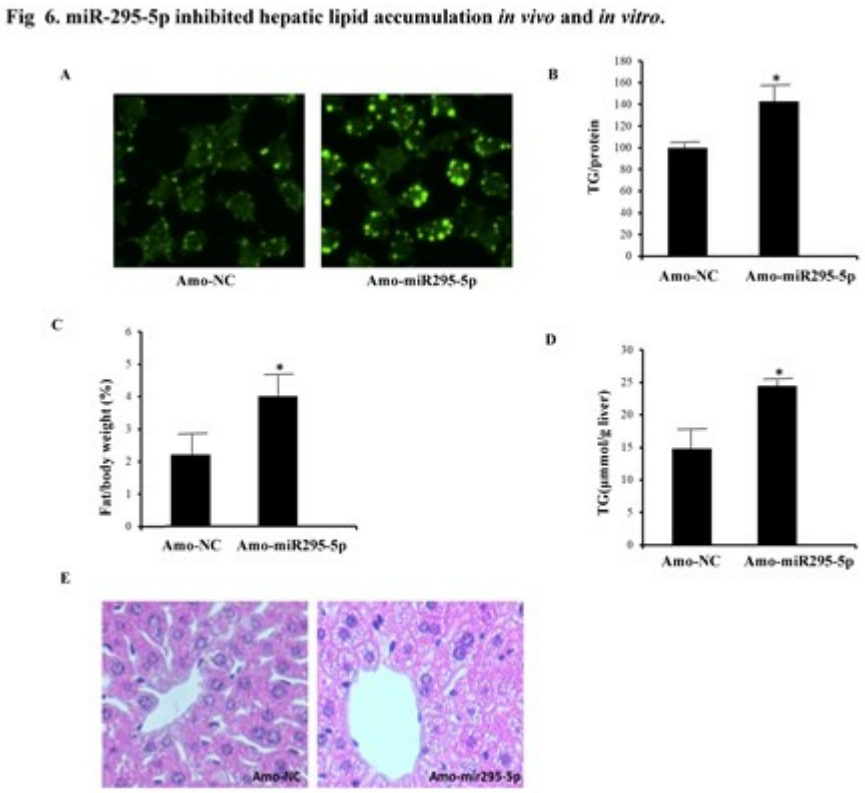

Fig 6. miR-295-5p inhibited hepatic lipid accumulation *in vivo* and *in vitro*.

(A) AML-12 cells were transfected Amo-NC or Amo-miR295-5p for 48h, and the intracellular intracellular lipid droplets were evaluated by fluorescence staining aasay.

(B) AML-12 cells were transfected with Amo-NC or Amo-miR295-5p for 48h, and triglyceride content was evaluated.

(C) Body fat mass ratio of C57/BL mice injected into the veins of the tails Amo-NC or Amo-miR295-5p after 10 weeks.

(D) The intracellular triglyceride in the liver of C57/BL mice injected into the veins of the tails Amo-NC or Amo-miR295-5p was evaluated.

(E) Representative photomicrographs of the H&E staining from liver sections in C57/BL mice injected into the veins of the tails Amo-NC or Amo-miR295-5p (10×20).

All the values are means ± SD from three separate experiments. *$P < 0.05$ compared with controls.

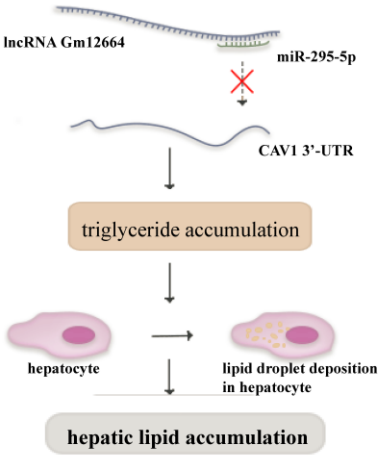

Fig 7. Graphical abstract of how long non-coding RNAs (lncRNAs) Gm12664 promotes hepatocellular lipid accumulation. Gm12664 sponges miR-295-5p to positively regulate CAV1 expression at the post-transcriptional level, and thereby promotes HFD-induced lipid accumulation in hepatocytes .

Fig 7. Graphical abstract of how lncRNA Gm12664 promotes hepatocellular lipid accumulation. Gm12664 sponges miR-295-5p to positively regulate CAV1 expression at the post-transcriptional level, and thereby promotes HFD-induced lipid accumulation in hepatocytes.

Supplementary material

Supplementary Table 1

Table 1. Sequences of primers for qRT-PCR analysis.
F, forward; R, reverse; m, mouse; h, human

Gene		Sequence (5'-3')
MM9LINCRNAEXON11355	Forward	5′- AGCCCTACATTCCCAAGGAC -3′
	Reverse	5′- ACCTGAGCACCAACAGCAA -3′
ENSMUST00000119467	Forward	5′-AATCCTGGAGGTGATCCGAAG-3′
	Reverse	5′-CTGTGCTACCTCAAAGCTTGAG-3′
uc009kux.1	Forward	5′-CTGGCAACTGACAGAGGGAAC-3′
	Reverse	5′-CTCCTGTCCCTCCTTGCTTATC-3′
AK079756	Forward	5′-TGACAGGATTATTGCGAGTCC-3′
	Reverse	5′-CTTTGGCTTATGGCTCAGTGT-3′
AK044811	Forward	5′-GACCCGTGCCTTTGTTCATA-3′
	Reverse	5′-TGCTGTGTGTTGAGAGTGGA-3′
AK166199	Forward	5′-AATTGGGAGCTATGCCAGAC-3′
	Reverse	5′-ACCTCCTGCCCACATCTACA-3′
ENSMUST00000169557	Forward	5′-GCCACCAATCAAGAAAGGAC-3′
	Reverse	5′-TAGCCCAACAAAGGAGGATG-3′
ENSMUST00000119644	Forward	5′-ACCTCATCTTTCAGTGCCATAG-3′
	Reverse	5′-TCCTCCATTCTGTTCTTCTGG-3′
uc008wdh.1	Forward	5′-CTTGTTCAGCGCATCCTC-3′
	Reverse	5′-TTGCTGAAGTCTCATCGC-3′
NR_030719	Forward	5′- AGGCTGTCAGTGGTTGGCATTG-3′
	Reverse	5′- TGGCATAATCACCTCCTGCGTC-3′
uc007owq.1	Forward	5′-TGGCGTTCTTCATCCTTCCT-3′
	Reverse	5′-CGGCCGGTTGAATGTAATGT-3′
uc.119	Forward	5′- GCTGTACCACTGTGCCCTAA-3′
	Reverse	5′- TGGCTTTCTTAATTCTCCTGTG-3′
ENSMUST00000122102	Forward	5′- ACTCCTGCTCTGCCATCTG-3′
	Reverse	5′- AAGTTTCTGCCTTCGCTCAT-3′
AK046703	Forward	5′- CAGGAAGCAGGCACAAAGTA -3′
	Reverse	5′- ACAAAGGGTCAATGGGAGAA -3′
ENSMUST00000071162	Forward	5′-GCAAGCAATGGAGATCCCTGAG-3′
	Reverse	5′-TCCAGATGCCCATCTTACCAAG-3′
NR_030715	Forward	5′-TTACTGGTGACGCTGAATAG-3′
	Reverse	5′-TTGGTTCAGATTTCCCAGAG-3′
miR-U6	Forward	5′-GCTTCGGCAGCACATATACTA-3′
	Reverse	5′-CGCTTCACGAATTTGCGTGTC-3′
miR-183-5p	Forward	5′-GCTTCGGCAGCACATATACTA-3′
	Reverse	5′-CGCTTCACGAATTTGCGTGTC-3′
miR-881-5p	Forward	5′-GGGGCAGAGAGATAACAGTCACATCT-3′
	Reverse	5′-ATCCAGTGCGTGTCGTGGA-3′
miR-295-5p	Forward	5′-GGGGACTCAAATGTGGGGCA-3′
	Reverse	5′-TCCAGTGCGTGTCGTGGA-3′
miR-155-3p	Forward	5′-GGGGCTCCTACCTGTTAGCATTAAC-3′
	Reverse	5′-GGGGCTCCTACCTGTTAGCATTAAC-3′
miR-222-3p	Forward	5′-AGCTACATCTGGCTACTGGGT-3′
	Reverse	5′-TATCCAGTGCGTGTCGTGG-3′

Supplementary Table 2

Table 2. An integrated analysis of LncRNA and mRNA expression based LncRNAs and mRNAs microarrays.

microarrays	lncRNAs	mRNA (up↓, down↑)	Length (bp)	Function
DOWN	NR_030715	Derl3 ↑、Hsd17b6↓	3418	endoplasmic reticulum, integral component of membrane, endoplasmic reticulum, oxidoreductase activity
	ENSMUST00000071162	Xlr3c ↓、Cyp3a16↓、Cyp3a41b↓	1131	meiotic cell cycle, monooxygenase activity
	ENSMUST00000119644	Sirpb1a↑、Xlr3a↓、Dkk4↑	682	tyrosine protein phosphatase , extracellular region
	Uc009kux.1	Xlr3a↓、Marco↓、Tnf↓、Capn8↑	1564	meiotic cell cycle, calcium-dependent cysteine-type endopeptidase activity
	NR_030719	Ugt1a9↓	3418	Starch and sucrose metabolism
	ENSMUST00000122102	Dpt↓	648	dipeptidyl-peptidase activity
	ENSMUST00000119467	LOC100038947↓	1274	regulation of inflammatory response to antigenic stimulus
UP	AK044811	Xlr3b↓、Hsd17b6↓、Derl3↑	886	meiotic cell cycle, retinol dehydrogenase activity, integral component of membrane, integral component of membrane
	Uc008wdh.1	Hsd17b6↓	1547	retinol dehydrogenase activity
	Uc007owq.1	Derl3↑、Cyp3a41a↓	1495	monooxygenase activity, integral component of membrane
	AK046702	Hsd17b6↓、Cyp3a41b↓	3177	monooxygenase activity
	Uc007vdz.1	Cyp3a44↓、Serpina9↑	3892	monooxygenase activity, serine-type endopeptidase inhibitor activity
	AK079756	Sirpb1a↓、Cyp3a11↓	1329	Steroid hormone biosynthesis, monooxygenase activity
	ENSMUST00000152600	Xlr3a↓、Serpina9↑、Xlr3a↓	421	meiotic cell cycle, serine-type endopeptidase inhibitor activity
	MM9LINCRNAEXON11355	Xlr3a↓、Serpina9↑、Cyp3a13↓	1082	meiotic cell cycle, monooxygenase activity, serine-type endopeptidase inhibitor activity
	Gm12664	Cd74↓、CAV1↑	913	prostaglandin biosynthetic process, lipoprotein metabolism
	AK166199	Marco↓、Capn8↓、Twist1↓	1351	G protein-coupled receptor binding, calcium-dependent cysteine-type endopeptidase activity, negative regulation of transcription by RNA polymerase II
	Uc.119	Twist1↓、Marco↓、Tnf↓	1523	G protein-coupled receptor binding, negative regulation of transcription by RNA polymerase II
	ENSMUST00000169557	Capn8↓、Twist1↓、Marco↓	4085	G protein-coupled receptor binding, negative regulation of transcription by RNA polymerase II